



Comparative Analysis of K-Means Clustering and Watershed Segmentation Techniques for Brain Tumor Detection in MRI

Ayesha Khan¹

¹Department of Computer Science & IT, The Islamia University of Bahawalpur, Pakistan.

Article Information

ABSTRACT

Article Type: Research Article

Copyright:

This work is licensed under creative common licensed and ©2024 All rights reserved United Frontiers Publisher

Corresponding Author:

ORCID 0009-0006-1425-429X

This study aims to evaluate and compare the efficiency of two segmentation techniques, K-Means clustering, and Watershed segmentation, in the detection of brain tumors using MRI scans. Accurate segmentation of brain MRI images is crucial for the diagnosis and treatment of brain tumors. Numerous techniques have been employed for this purpose, but a clear comparison between these methods remains underexplored. This research provides a comparative analysis of K-Means clustering and Watershed segmentation to identify the superior technique for brain tumor detection. The study utilized MRI scans of patients with three different brain diseases: metastatic bronchogenic carcinoma, anaplastic astrocytoma, and sarcoma. Morphological operations were applied for skull removal, followed by segmentation into gray matter (GM), white matter (WM), cerebrospinal fluid (CSF), and tumor areas using both K-Means clustering and Watershed segmentation. The segmented regions were quantified, and the efficiency of each technique was assessed through percentage calculations and visual representation via pie charts. The results indicate that K-Means clustering outperforms Watershed segmentation in accurately identifying and segmenting the tumor areas as well as the GM, WM, and CSF regions. For metastatic bronchogenic carcinoma, K-Means detected an average tumor area of 12.74%, compared to Watershed's 6.99%. Similar trends were observed for anaplastic astrocytoma and sarcoma, with K-Means consistently providing higher accuracy and clearer segmentation boundaries. K-Means clustering proves to be a more effective technique for brain tumor detection and segmentation in MRI scans compared to Watershed segmentation. The superior performance of K-Means is attributed to its ability to classify regions without the limitations associated with the structuring elements required by Watershed segmentation. Future research should further refine these techniques and explore their integration into automated diagnostic systems.

Key Words

Gray Matter (GM), White Matter (WM), Cerebrospinal fluid (CSF), Tumor, magnetic resonance imaging (MRI), Watershed Algorithm, K-Means, Clustering, Segmentation.

1. INTRODUCTION

There are many researches about the segmentation of Brain MRI along with many techniques are experienced but there is no any clear comparison between the techniques to find out the best technique. This research is about the Brain MRI segmentation for Tumor detection along with the comparison between two techniques which are k-Means clustering and Watershed segmentation. The system's input is Brain MRI of the patients of Brain tumor. Three diseases are examined in the system for the clarity of results. Morphological operations have been used for the removal of skull in the Brain MRI from main part of the Brain. The process is continued with the segmentation of the Brain into four parts as White matter (WM), Gray Matter (GM), Cerebrospinal Fluid (CSF), and Defected area though both techniques. Then system will calculate the defected area and mark the boundary of the tumor area in the Brain MRI. For the comparison of the technique's percentages will be calculated of WM, GM, CSF and tumor to present the difference and efficiency of the better technique. Result of tumor area and comparison between techniques shown by pie charts. Fig 1 shows the block diagram of system.

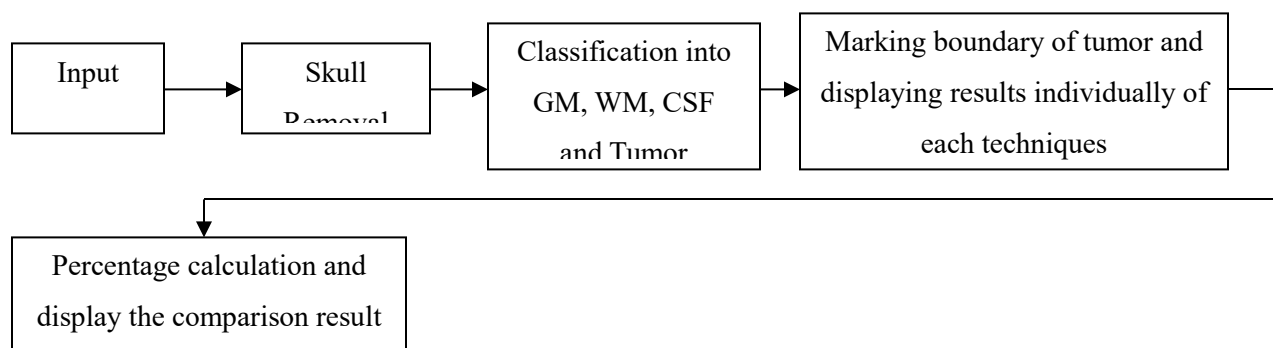


Fig 1: Block Diagram of System

2. Material and Method

2.1 Literature Review

Implementation of a neuro-fuzzy segmentation process of the MRI data is presented in the study to detect various tissues like white matter, gray matter, CSF and tumor. The advantage of hierarchical self-organizing map and fuzzy c means algorithms are used to classify the image layer by layer. The lowest level weight vector is achieved by the abstraction level. This has also achieved a higher value of tumor pixels by this neuro-fuzzy approach. Neuro fuzzy technique shows that MRI brain tumor segmentation using HSOM-FCM also perform more accurate one (1).

Peak detection technique was used to generate the contour lines of the tumor area in the image of a brain slice. The tumor area was scanned and correlated with a reference image. The resultant cross correlation was plotted with respect to spatial coordinates. The peak values represented the normal and tumor tissue transitions and they were plotted in contour form to define the outlines of the tumor area (2).

Another efficient method for automatic brain tumor segmentation for the extraction of tumor tissues from MR images, it combines Perona and Malik anisotropic diffusion model for image enhancement and Kmeans clustering technique for grouping tissues belonging to white matter, gray matter, CSF and tumor. The proposed method uses T1, T2 and PD weighted gray level intensity images (3).

Some other research is Spatial normalization and segmentation of infant brain MRI data based on adult or pediatric reference data may not be appropriate due to the developmental differences between the infant input data and the reference data. In this study, have constructed infant templates and a priori brain tissue probability maps based on the MR brain image data from 76 infants ranging in age from 9 to 15 months. They employed two processing strategies to construct the infant template and a priori data: one processed with and one without using a priori data in the segmentation step. Using the templates, comparisons between the adult templates and the new infant templates are presented. Tissue distribution differences are apparent between the infant and adult template, particularly in the gray matter (GM) maps. The infant a priori information classifies brain tissue as GM with higher probability than adult data, at the cost of white matter (WM), which presents with lower probability when compared to adult data. The differences are more pronounced in the frontal regions and in the cingulated gyrus. Similar differences are also observed when the infant data is compared to a pediatric (age 5 to 18) template. The two-pass segmentation approach taken here for infant T1W brain images has provided high quality tissue probability maps for GM, WM, and CSF, in infant brain images (4).

Computer Aided Detection System (CAD) is used to detect tumor in Brain MRI automatically in research. Mainly, Image enhancement and brain segmentation steps are studied in this research (5).

Fuzzy classification, symmetry analysis and spatially constrained deformable models are used in the investigation to segment the brain from 3D images. The main preference is of segment then to detect tumor through selecting asymmetric areas with respect to the approximate brain symmetry plane and fuzzy classification (6).

2.2 Brain Images

The technique which is commonly used in radiology as a primarily imaging methodology for medical use in visualizing the function, hard and soft tissues of body is Magnetic resonance imaging (MRI). In the comparison of computed tomography (CT) Scan, the MRI provides greater contrast between body's soft tissues in different parts. MRI uses the strong magnetic field which is used to align the nuclear magnetization in atoms of hydrogen in water in the body but not like CT scan which uses ionizing radiation (7). Whereas, MRI normally provides the 2-dimensional images but for some cases MRI can be used to generate 3 dimensional images (8). MRI is also used for the sensitive parts of the body as heart, eye and brain.

MRI has many capturing techniques like T1, T2 weighted and proton density. Different tissues are captured by different techniques depends upon the part of body. Whereas, T1 weighted gives better contrast of gray matter and white matter, while T2 weighted are suitable for edema which is sensitive to water content and gives the better and enhanced contrast of GM and WM (9). Another technique called T2* weighted increased the contrast of certain kind of tissues which are venous blood. It is good in present the flow of blood and visualizing the blood (10). The capturing technique which is the input of this system is T2 Weighted with the plane of Axial.

At least ten images of three different diseases are used for the system to test and efficiency and difference between k-Mean and Watershed segmentation. MRI's are taken from the library of Harvard University "The Whole Brain Atlas" (11). Samples MRI are shown in Fig 2 below.

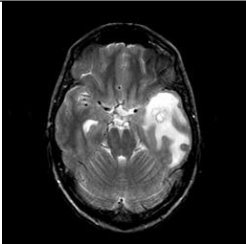
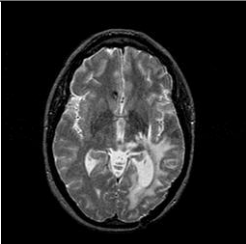
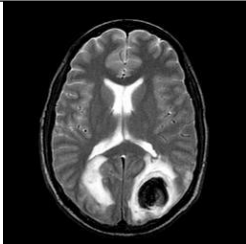
		
(i)Disease1:Metastatic bronchogenic carcinoma (12)	(ii)Disease2:Anaplast Astrocytoma (13)	(iii)Disease3: Sarcoma (14)

Fig 2: Three Diseases used to test the system by "The Whole Brain Atlas" (11)

2.3 Methodology

As discussed above, the study uses MRI of Brain for the input of the system. The MRI contains the skull part in it and for the processing the skull have to be removed first from the Brain area. Morphological operations of digital image processing are used for removing the skull from the brain.

2.3.1 Morphological Operations

Erosion and dilation methods are used for skull removal. Erosion is used to erode the binary or grayscale image and retrieve the eroded image as a result. A structuring element needs to be applying on the inputted image or MRI to gain the required purpose. A Structuring element is the matrix made of zeros and ones according to the shape and need of the image. Equation 1: shows the formula use for the erosion process.

$$A \ominus B = \{Z \in \varepsilon | B_z \subseteq A\} \quad \dots \text{Equation 1}$$

A is the name given to the inputted MRI which has to be erode and B represents the structuring element (15).

Dilation process is same as erosion. Dilation is used to recover the important holes and missing parts lost by the process of erosion. Dilation is use to grow or thicken the edge and parts of the image. Mathematically Dilation is represented in Equation 2:

$$A \oplus B = \{Z \in \varepsilon | B_z \subseteq \theta\} \quad \dots \text{Equation 2}$$

Where A again symbolizes the inputted image and B is structuring element (15).

The study use fixed along with user flexible structuring element. The Structuring element can be change using GUI of the study. The result of the erosion function on the original image is as bellow in Fig 3:



Fig 3: Applying Erosion on Original MRI

After applying erosion, dilation is applied to retrieve the side effects of erosion (lost data from brain part). The Result of dilation function is represented in Fig 4:



(i) Original MRI	(ii) Dilated MRI
------------------	------------------

Fig 4: Applying Dilation on Eroded MRI

After removing skull, process proceeds with segmentation into four part WM, GM, CSF and Tumor through k-Means clustering and afterwards Watershed for comparison.

2.3.2 K-Means Clustering

K-Means is a clustering technique to group or classification of K number groups based on the attributes of the objects. K-Means clustering work by calculating the distance between the objects and classify the objects in one group who have minimum distance in between. Moreover if the data is bigger than K numbers of clusters then calculate the centroid and then calculate the minimum distance of objects of each centroid. The data is said to be of the group which has the minimum distance. The calculation of centroids and objects minimum distance is calculated continuously until every object moved to its specific classification (16). The brain MRI is divided into four classification as WM, GM, CSF and defected area. Fig 5 represents the clusters obtained by K-Means clustering.


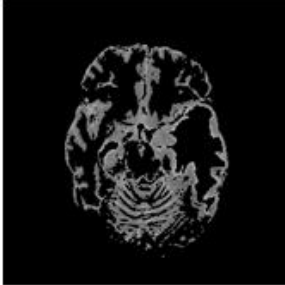
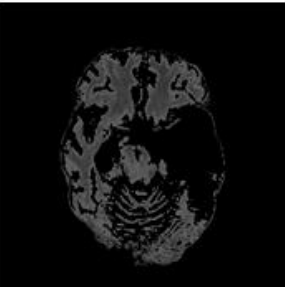

 <p>objects in cluster 1 "Tumor Area"</p>	 <p>objects in cluster 2 "White Matter (WM)"</p>
(i) Defected Area	(ii) White Matter (WM)
 <p>objects in cluster 3 "Gray Matter (GM)"</p>	 <p>objects in cluster 4 "Cerebrospinal Fluid (CSF)"</p>
(iii) Gray Matter (GM)	(iv) Cerebrospinal fluid (CSF)

Fig 5: Segments through K-Means

2.3.3 Watershed Segmentation

The morphological based segmentation of the image is Watershed segmentation. The method is normally used to preprocess the grayscale image. Watershed works with the difference of

high valued pixel and low valued pixel (15). A gradient magnitude is used as the tomography surface of the image in Watershed classification. There are different ways of lines of watershed. If the gradients of images are estimated correctly gives the best result in dividing into classifications (17) . Segmented parts are the result of watershed segmentation. Moreover, there are three techniques used in watershed segmentation which are distance transform, gradient and marker-controlled watershed. The technique used in the study is Watershed segmentation through gradients. The Fig 6 shows the segmentation of MRI using Watershed.

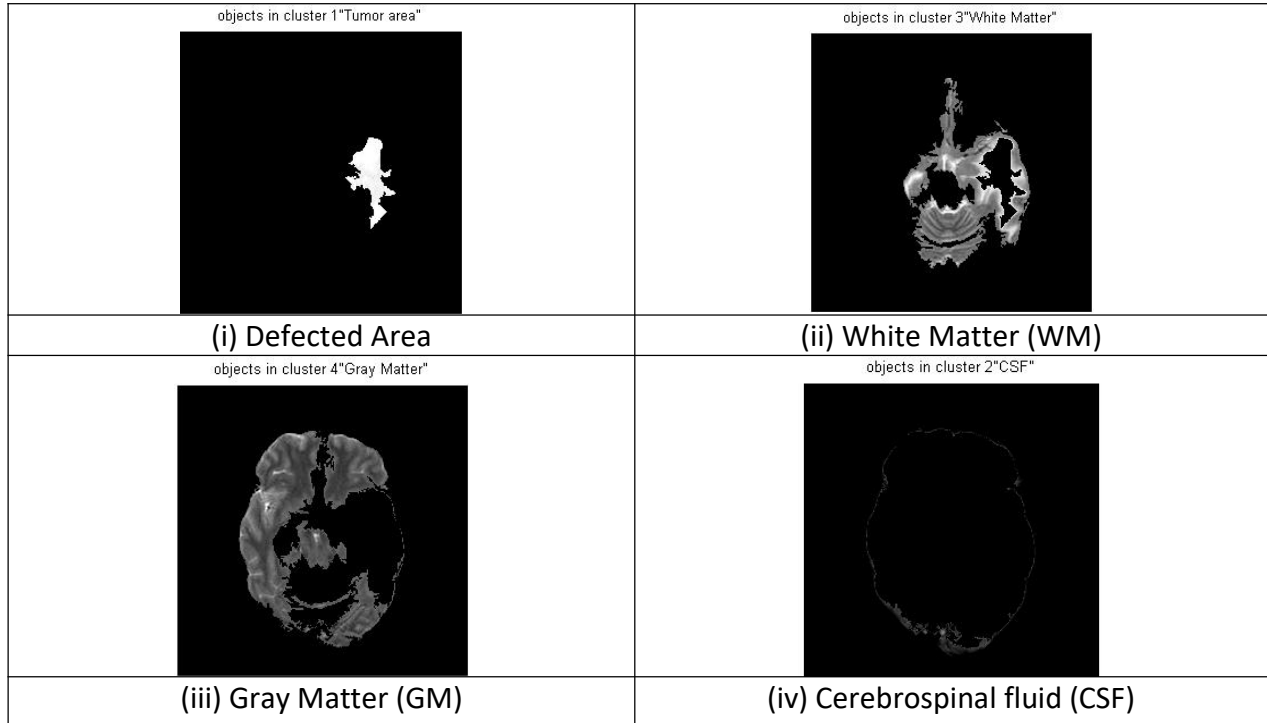
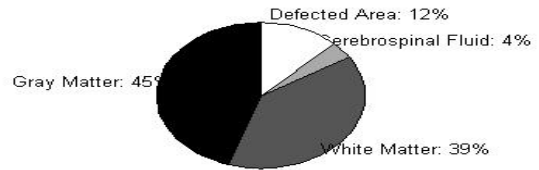
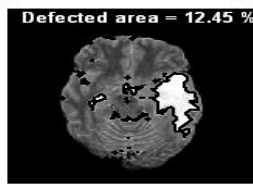


Fig 6: Segments through Watershed

Comparison between k-Means and Watershed

After segmentation study calculates the percentage of defeated area detected by both techniques along with WM, GM and CSF. The results are shown in pie charts n Fig 7.

Brain image detected through k-Means



Brain image detected through Watershed

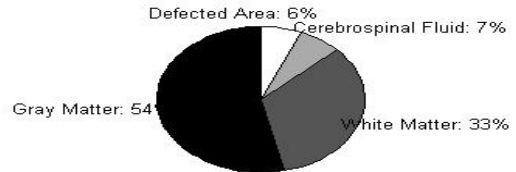
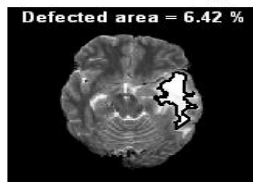


Fig 7: Comparison between k-Means and Watershed

3. Results

Through the test of data set taken from the “The Whole Brain Atlas”, the study’s result is in the favor of k-Means clustering as a better technique for segmentation and tumor detection. Ten images of each disease are examined in the system for calculating the total and average of defected area, GM, WM and CSF.

3.1 Metastatic bronchogenic carcinoma

Data of three patients is taken for test. First is Metastatic bronchogenic carcinoma. The patient used to be addict of tobacco from a long period and then start suffering from headaches duration of one month before the MRIs were taken. The patient found in trouble in words she speaks (12). The Table 1 represents the percentage of GM, WM, CSF and defected area via watershed.

Images Sr. No.	Gray Matter	White Matter	CSF	Defected Area
1	12.3013	67.70546	11.66353	8.32971
2	53.5788	33.44695	6.552157	6.422101
3	81.89831	7.754216	3.291603	7.055868
4	28.64213	62.20004	2.487004	6.670826
5	85.45538	7.711857	2.633114	4.19965
6	63.09988	27.13668	2.74292	7.020519
7	14.4742	71.54801	3.156978	10.82081
8	80.1285	10.28414	3.791512	5.795856
9	11.72198	77.05628	4.050024	7.171717
10	53.5788	33.44695	6.552157	6.422101
Total	484.8793	398.29058	46.921	69.90916

Average	48.48793	39.829058	4.6921	6.990916
----------------	-----------------	------------------	---------------	-----------------

Table 1: Disease 1 results through Watershed

Whereas, in Table 2 k-Means represent better results as compares to Watershed.

Images Sr. No.	Gray Matter	White Matter	CSF	Defected Area
1	42.45543	39.537131	5.276127	12.73131
2	45.01301	38.963136	3.569827	12.45403
3	48.13916	35.662579	2.201499	13.99676
4	51.89021	29.028904	1.854855	17.22603
5	53.92884	27.256062	1.816515	16.99858
6	57.84721	24.639647	2.107004	15.40614
7	55.48879	26.566514	2.442848	15.50185
8	61.4605	25.522577	2.750882	10.26604
9	60.60606	30.4329	2.457912	6.503127
10	53.84049	35.552159	4.296145	6.311202
Total	530.6697	313.16161	28.77361	127.3951
Average	53.06697	31.316161	2.877361	12.73951

Table 2: Disease 1 results through k-Means

3.2 Anaplastic Astrocytoma

Secondly disease two is Anaplastic Astrocytoma. The patient is 51 years old and experiencing the hemi-paresis in right side and visual loss (13). Table 3 contains the results calculated from watershed.

Images Sr. No.	Gray Matter	White Matter	CSF	Defected Area
1	5.79123281	75.24103	5.546985	13.42075
2	2.63812304	68.73175	3.654449	24.97567
3	0.99025464	72.45625	3.992455	22.56104
4	30.8217771	45.04879	3.251156	20.87827
5	10.4969007	65.06453	2.91637	21.5222
6	24.4512532	49.63584	3.315084	22.59782
7	24.4512532	49.63584	3.315084	22.59782
8	24.4512532	49.63584	3.315084	22.59782
9	24.4512532	49.63584	3.315084	22.59782
10	13.1140864	67.34715	2.652344	16.88642
Total	161.657388	592.4329	35.27409	210.6356
Average	16.1657388	59.24329	3.527409	21.06356

Table 3: Disease 2 results through Watershed

Where, Table 4 represents same dataset through k-Means.

Images Sr. No.	Gray Matter	White Matter	CSF	Defected Area
1	48.065304	26.50084	3.914385	21.51948
2	47.7619202	24.48913	2.573251	25.17569
3	45.9813476	25.72566	3.154144	25.13885
4	47.6065742	22.49615	2.634823	27.26246
5	53.4600142	22.48755	2.301595	21.75084
6	53.6541263	26.01838	2.250239	18.07725
7	53.6541263	26.01838	2.250239	18.07725
8	53.6541263	26.01838	2.250239	18.07725
9	53.6541263	26.01838	2.250239	18.07725
10	51.7916457	30.19124	2.365375	15.65174
Total	509.283311	255.9641	25.94453	208.8081
Average	50.9283311	25.59641	2.594453	20.88081

Table 4: Disease 2 results through k-Means

3.3 Sarcoma

Thirdly, the disease third is Sarcoma. The patient was of 22 years and suffered Ewing's sarcoma (14). Again Table 5 shows results from watershed.

Images Sr. No.	Gray Matter	White Matter	CSF	Defected Area
1	38.7814506	54.77092	3.792017	2.655608
2	79.3366757	12.58002	3.050521	5.032781
3	44.0543341	15.42919	6.477111	34.03937
4	15.2797534	64.87672	4.634898	15.20863
5	33.0412617	48.17588	2.700335	16.08252
6	27.8912124	52.93127	2.777207	16.40031
7	52.5861699	24.16191	4.026269	19.22565
8	38.6842226	45.85952	4.440978	11.01528
9	25.3593991	25.80709	7.202905	41.6306
10	27.4919614	45.00938	12.96222	14.53644
Total	382.506441	389.6019	52.06446	175.8272
Average	38.2506441	38.96019	5.206446	17.58272

Table 5: Disease 3 results through Watershed

Now, Table 6 shows calculation through k-Means

Images Sr. No.	Gray Matter	White Matter	CSF	Defected Area
1	52.6855138	36.21357	2.643646	8.457275

2	52.0208253	33.89125	2.364057	11.72387
3	52.219792	32.01719	3.38053	12.38249
4	51.0589537	31.25494	3.161056	14.52505
5	54.046519	25.9957	2.50916	17.44862
6	54.1473234	28.79915	1.943223	15.11031
7	55.659527	30.27858	2.347942	11.71395
8	50.5574162	34.40382	2.954535	12.08423
9	48.4156594	36.53186	4.342635	10.70984
10	48.1798109	35.85461	5.786107	10.17947
Total	518.991341	325.2407	31.43289	124.3351
Average	51.8991341	32.52407	3.143289	12.43351

Table 5: Disease 3 results through k-Means

By the thorough study of the results, there is a clear difference in between the average and total amount of GM, WM, CSF and defected through Watershed and k-Means clustering. Watershed segmentation lacks in providing the proper calculation of gray matter and white matter. Some area of the defected part is also missing in watershed segmentation but k-Means providing the better results in every segment GM, WM, CSF and defected area. K-Means is successful in providing the approximate values of GM and WM containing in MRI along with the defected area.

4. Discussion

As considering the results watershed segmentation failed to segment the gray matter and white matter properly. Moreover, the defected are which is not joint to another defected area in same MRI is also missing when detection technique is watershed. While comparing the watershed technique with k-Means the study found that k-Means has the added benefit of separating gray matter and white matter properly. The two defected areas which are apart from bigger area in same MRI are easily detected by k-Means.

The noticed limitation with watershed segmentation is its method of using structuring element for classification. The structuring element used in the study is same for every image but watershed do not support same structuring element for every image. Let see in Fig 9, there is the representation of different structuring element on same image which provide the clear difference. And Fig 10 shows the same structuring element but different image.

Where, Fig 8 contain the original image which being processed.

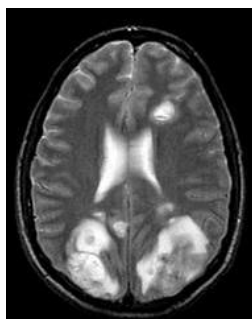


Fig 8: Original MRI (14)

(i) Defected area	(ii) White Matter	(iii) Gray Matter

Fig 9: Segments through Watershed using same Structuring Element

(i) Defected area	(ii) White Matter	(iii) Gray Matter

Fig 10: Segments through Watershed using Different Structuring Element and same image

Considering both Figs 9 and 10 there s a clear difference between segments extracted through watershed. In Fig 9 defected area is not completed segmented and the gray matter is still present in the white matter segment image. For overcome the difference by changing only 2 points in structuring element provide more accurate defected area but problem increases in white matter and gray matter segments. Still some of the defected are left from segmented to defected area and it is still the part of white matter in the figure. Furthermore, Fig 11 shows the segments of same image through k-Means clustering and the results are clear. The defected are is clearly and accurately separated from the remaining brain part. There is no limitation of structuring element in k-Means clustering. This provides the clarity of efficiency of k-Means clustering technique over Watershed segmentation.

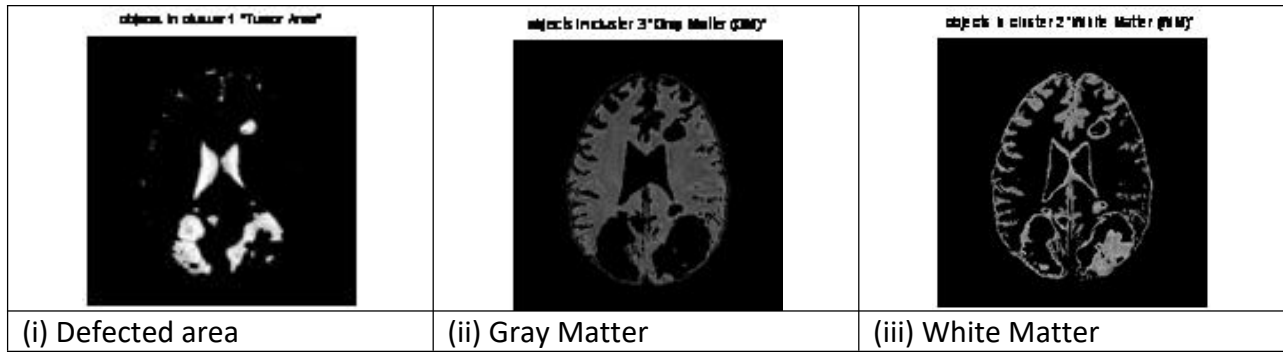


Fig 11: Segments through K-Means on the same Image

The charts below show the clear difference of both techniques. Charts are building by using total and average of all three diseases regarding segments which are GM, WM, CSF and defected area. The chart shows that K-Means extract the groups of same kind of data accurately but watershed has the limitations in segmentations. It failed to provide the clear distinction between segments. Watershed missed a number of data regarding gray matter or white matter and mixed up the gray matter in white and defected area in white matter each does not provide the accurate or approx total and average data. Hence this proves that K-Means is a better techniques for segmentation regarding this study.

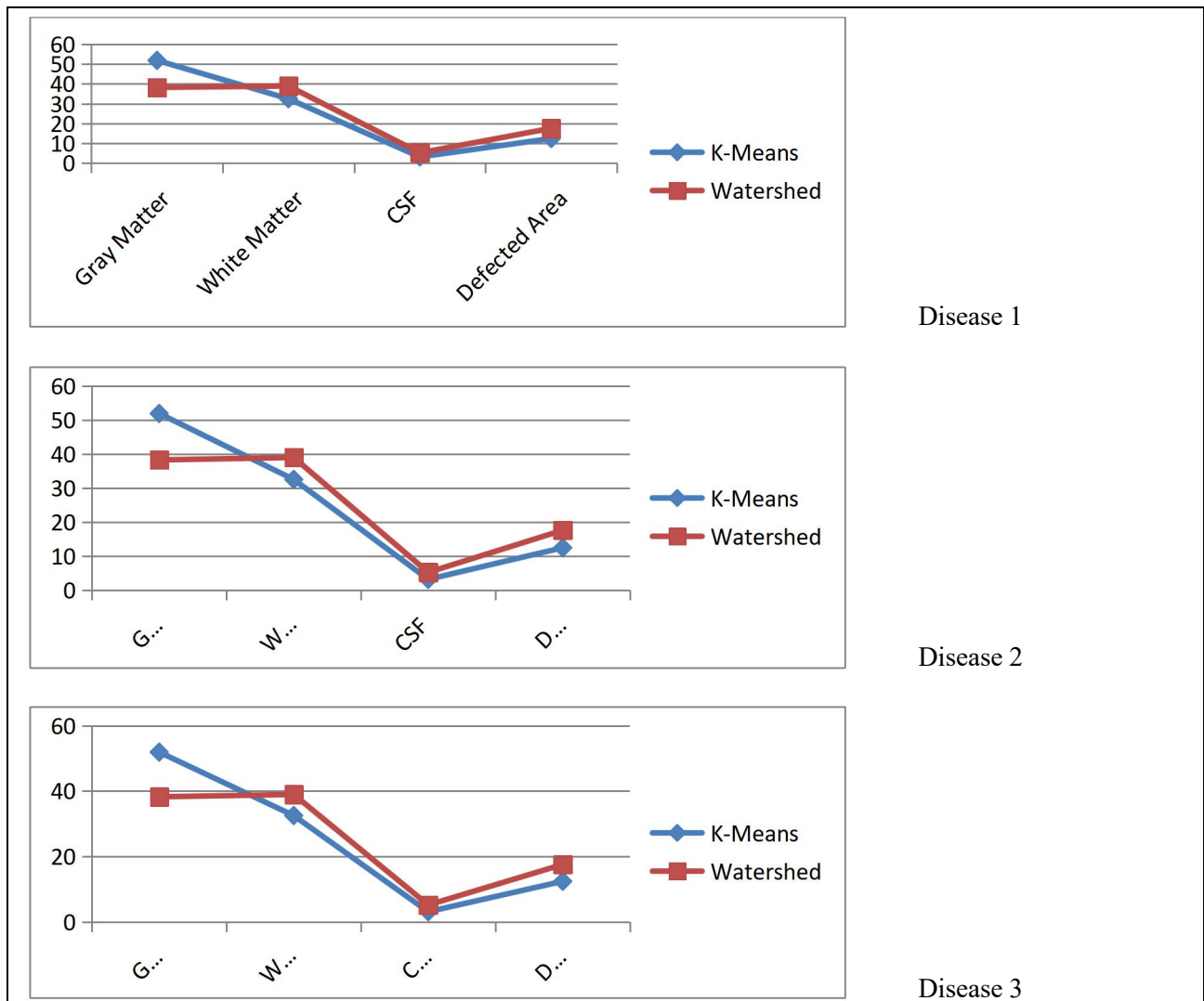


Fig 12: Chart shows the difference between K-Means and Watershed

5. Conclusion

As the study is conducted to find out the better technique for detecting tumor through Brain MRI, the results and discussion sessions provides the detail explanation about K-Means as the better techniques over watershed. K-Means is proved as the efficient method of segmentation. K-Means covers more and accurate area of GM, WM, CSF and defected area rather than watershed. There is no limitation of structuring element in K-Means and it works the same for every image them watershed segmentation.

Author contributions: All authors equally contributed to this study

Competing Interests: The author declares that this work has no competing interests.

Grant/Funding information: The author declared that no grants supported this work.

Data Availability Statement: The associated data is available upon request from the corresponding author.

References

- [1] Jaspars M, Pascale DD, et al. The marine biodiscovery pipeline and ocean medicines of tomorrow. *Journal of the Marine Biological Association of the United Kingdom*, 2016, 96(1): 151–158.
- [2] Hasan S, Ansari IM, et al. Major bioactive metabolites from marine fungi: A review. *Bioinformation*, 2015, 11(4): 176–181.
- [3] Snelgrove PV. An ocean of discovery: Biodiversity beyond the census of marine life. *Planta Medica*, 2016, 82(9-10): 790–799.
- [4] Torres RV, Encinar AJ, et al. An updated review on marine anticancer compounds: The use of virtual screening for the discovery of small-molecule cancer drugs. *Molecules*, 2017, 22(7): 1037.
- [5] Sawadogo W, Boly, et al. A survey of marine natural compounds and their derivatives with anti-cancer activity reported in 2012. *Molecules*, 2015, 20: 7097–7142.

- [6] Shaden AM, Khalifa, et al. Marine natural products: A source of novel anticancer drugs. *Marine Drugs*, 2019, 17(9): 491.
- [7] Dyshlovoy AS, Honecker F, Marine compounds and cancer: The first two decades of XXI century. *Marine Drugs*, 2020. 18(1): 20.
- [8] Giordano D, Coppola D, et al. Marine microbial secondary metabolites: Pathways, evolution and physiological roles. *Advances in Microbial Physiology*, 2015, 66: 357–428.
- [9] Srinivasan R, Kannappan A, et al. Marine bacterial secondary metabolites: A treasure house for structurally unique and effective antimicrobial compounds. *Marine Drugs*. 2021.
- [10] Townsend M, Davies K, et al. The challenge of implementing the marine ecosystem service concept. *Frontier in Marine Sciences*, 2018, 5: 359.
- [11] Corinaldesi C. New perspectives in benthic deep-sea microbial ecology. *Frontiers in Marine Sciences*, 2015, 2: 17.
- [12] Cochrane SKJ, Andersen JH, et al. What is marine biodiversity? Towards common concepts and their implications for assessing biodiversity status. *Frontier in Marine Sciences*, 2016, 3: 248.
- [13] Hegazy, M.E.F, Mohamed, T.A, et al. Molecular architecture and biomedical leads of terpenes from red sea marine invertebrates. *Marine Drugs* 2015, 13, 3154–3181.
- [14] Singh, R.P, Kumari, P, et al. Antimicrobial compounds from seaweeds-associated bacteria and fungi. *Applied Microbial Biotechnology* 2015, 99, 1571–1586.
- [15] Malve H. Exploring the ocean for new drug developments: Marine pharmacology. *Journal of Pharmacy and Bioallied Sciences*, 2016, 8(2): 83–91.
- [16] Petersen EL, Kellermann YM, et al. Secondary metabolites of marine microbes: From natural products chemistry to chemical ecology Youmarase 9-The oceans: Our research, Our future, 2019: 159–180.
- [17] Calle LD. Marine microbiome as source of natural products. *Microbial Biotechnology*, 2017, 10(6): 1293–1296.
- [18] Khalifa SAM, Elias N, et al. Marine natural products: A source of novel anticancer drugs. *Marine Drugs*, 2019, 17(9): 491.
- [19] Romano G, Costantini M, et al. Marine microorganisms as a promising and sustainable source of bioactive molecules. *Marine Environmental Research*, 2017, 128: 58–69.
- [20] Tortorella E, Tedesco P, et al. Antibiotics from deep-sea microorganisms: Current discoveries and perspectives. *Marine Drugs*, 2018, 16(10): 355.
- [21] Choudhary A, Naughton ML, et al. Current status and future prospects of marine natural products (MNPs) as antimicrobials. *Marine Drugs*, 2017, 15(9): 272.
- [22] Daniel A, Dias A, et al. A historical overview of natural products in drug discovery. *Microorganisms*, 2012, 2(2): 303–336.
- [23] Burkholder PR, Pfister MR, et al. Production of a pyrrole antibiotic by a marine bacterium. *Applied Microbiology*, 1966, 14 (4): 649–653.
- [24] Waters AL, Hill RT, et al. The expanding role of marine microbes in pharmaceutical development. *Current Opinion Biotechnology*, 2010, 21(6): 780–786.
- [25] Ameri A. Marine microbial natural products. *Jundishapur Journal of National Pharmaceutical Products*, 2014, 9(4): e24716.
- [26] Xiong ZQ, Wang JF, et al. Recent advances in the discovery and development of marine microbial natural products. *Marine Drugs*, 2013, 11(3): 700–717.
- [27] Xiong ZQ, Wang JF, et al. Recent advances in the discovery and development of marine microbial natural products. *Marine Drugs*, 2013, 11(3): 700–717.

- [28] Gunathilake VK. Marine bacteria and fungi as sources for bioactive compounds: Present status and future trends. *International Journal of Advanced Research*, 2017, 5(9): 1–5.
- [29] Hou XM, Hai Y, et al. Chemical and bioactive marine natural products of coral-derived microorganisms (2015-2017). *Current Medicinal Chemistry*, 2019, 26(38): 6930–6941.
- [30] Bhatia KS, Bhatia KR, et al. Biotechnological potential of microbial consortia and future perspectives. *Critical Reviews in Biotechnology*, 2018, 38(8): 1209–1229.
- [31] Blunt, JW, Copp BR, et al. Marine natural products. *Natural Products Reports*, 2014, 31: 160–258.
- [32] Romanenko LA, Uchino M, et al. Occurrence and antagonistic potential of *Stenotrophomonas* strains isolated from deep-sea invertebrates. *Achieves of Microbiology*, 2008, 189(4): 337–344.
- [33] Caulier S, Nannan C, et al. Overview of the antimicrobial compounds produced by members of the *Bacillus subtilis* group. *Frontier Microbiology*, 2019, 10: 302.
- [34] Kalyani. P, Hemalatha. K, et al. Review paper-Marine microbial bioactive compounds. *International Journal of Engineering Sciences and Research Technology*, 2016, 5(11): 124–133.
- [35] Alves C, Silva J, et al. From marine origin to therapeutics: The antitumor potential of marine algae-derived compounds. *Frontier Pharmacology*, 2018, 9: 777.
- [36] Andryukov B, Mikhailov V, Besednova N. The biotechnological potential of secondary metabolites from marine bacteria. *Journal of Marine Sciences and Engineering*, 2019, 7: 176.
- [37] Sharma S, Fulke BA, et al. Bioprospection of marine actinomycetes: recent advances challenges and future perspectives. *Acta Oceanologica Sinica*, 2019, 38(6): 1–17.
- [38] MaySubramani R, Sipkema D, et al. Marine rare actinomycetes: A promising source of structurally diverse and unique novel natural products. *Marine Drugs*, 2019, 17(5): 249.
- [39] Leach BE, Calhoun KM, et al. Chartreusin, a new antibiotic produced by *Streptomyces chartreusis*, a new species. *The Journal of the American Chemical Society*, 1953, 75(16): 4011–4012.
- [40] Zotchev S, Haugan K, et al. Identification of a gene cluster for antibacterial polyketide-derived antibiotic biosynthesis in the nystatin producer *Streptomyces noursei* ATCC 11455. *Microbiology*, 2000, 146(3): 611–619.
- [41] Hartsel S, Bolard J, Amphotericin B: new life for an old drug. *Trends in Pharmacological Sciences*, 1996, 17(12): 445–449.
- [42] Sharma M, Dangi P, et al. Actinomycetes: source, identification, and their applications. *International Journal of Current Microbiology and Applied Sciences*, 2014, 3(2): 801–832.
- [43] Li S, Tian X, et al. Antimycins from marine *Streptomyces* sp. SCSIO 1635 from the South China Sea. *Natural Product Research and Development*, 2011, 23(1): 10–14.
- [44] Maskey RP, Li FC, et al. Chandrananimycins A-C: production of novel anticancer antibiotics from a marine *Actinomadura* sp. isolate M048 by variation of medium composition and growth conditions. *The Journal of antibiotics*, 2003, 56(7): 622–629.
- [45] Pedersen JC. Natamycin as a fungicide in agar media. *Applied and Environmental Microbiology*, 1992, 58(3): 1064–1066.
- [46] Williams PG, Miller ED, et al. Arenicolides A-C, 26-membered ring macrolides from the marine actinomycetes *Salinispora arenicola*. *The Journal of Organic Chemistry*, 2007, 72(14): 5025–5034.
- [47] Kwon HC, Kauffman CA, et al. Marinomycins A-D, antitumor-antibiotics of a new structure class from a marine actinomycete of the recently discovered genus *Marinispora*. *Journal of the American Chemical Society*, 2006, 128(5): 1622–1632.
- [48] Schumacher RW, Talmage SC, et al. Isolation and structure determination of an antimicrobial ester from a marine sediment-derived bacterium. *Journal of Natural Products*, 2003, 66(9): 1291–1293.
- [49] Floss H G, Yu TW. Rifamycin-mode of action, resistance, and biosynthesis. *Chemical Reviews*, 2005, 105(2): 621–632.

- [50] Feitelson MA., Arzumanyan A, et al. Sustained proliferation in cancer: Mechanisms and novel therapeutic targets. *Seminars in Cancer Biology*, 2015, 35: S25–S54.
- [51] Dasari VR, Muthyala MK et al. Novel pyridinium compound from marine actinomycete, *Amycolatopsis alba* DVR D4 showing antimicrobial and cytotoxic activities in vitro. *Microbiological Research*, 2012, 167(6): 346–351.
- [52] Jørgensen H, Degnes KF, et al. Insights into the evolution of macrolactam biosynthesis through cloning and comparative analysis of the biosynthetic gene cluster for a novel macrocyclic lactam, ML-449. *Applied and Environmental Microbiology*, 2010, 76(1): 283–293.
- [53] Sato S, Iwata F, et al. Usabamycins A–C: new anthramycin-type analogues from a marine-derived actinomycetes. *Bioorganic & Medicinal Chemistry Letters*, 2011, 21(23): 7099–7101.
- [54] Li S, Tian X, et al. Antimycins from marine *Streptomyces* sp. SCSIO 1635 from the South China Sea. *Natural Product Research and Development*, 2011, 23(1): 10–14.
- [55] Hayakawa Y, Shirasaki S, et al. Structures of new cytotoxic antibiotics, piericidins C7 and C8. *The Journal of Antibiotics*, 2007, 60(3): 201–203.
- [56] Lopez PB, Pepper HB, et al. Biosynthetically guided structure-activity relationship studies of merochlorin A, an antibiotic marine natural product. *Chemistry Medicinal Chemistry*, 2017, 12(23): 1969–1976.
- [57] Bramhachari PV, Anju S, et al. Secondary metabolites from marine endophytic fungi: emphasis on recent advances in natural product research, In *Advances in Endophytic Fungal Research [B]*, Singh BP (Editor), Springer, 2019, pp 339–350.
- [58] Nicoletti R, Vinale F, et al. Bioactive compounds from marine-derived *Aspergillus*, *Penicillium*, *Talaromyces* and *Trichoderma* Species. *Marine Drugs*, 2018, 16(11): 408.
- [59] Jin L, Quan C, et al. Potential pharmacological resources: Natural bioactive compounds from marine-derived fungi. *Marine Drugs*, 2016, 14(4): 76.
- [60] Song T, Tang M, et al. Novel bioactive penicypyrroether A and pyrrospirone J from the marine-derived *Penicillium* sp. ZZ380. *Marine Drugs*, 2019, 17(5): 292.
- [61] Renato B, Nikolai M, et al. Marine-derived anticancer agents: Clinical benefits, innovative mechanisms, and new targets. *Marine Drugs*, 2019, 17(6): 329.
- [62] Barre LS, Bates SS. Bioactive metabolites and molecules: Blue Biotechnology: Production and use of marine molecules, John Wiley & Sons, 2018: 611–642.
- [63] Wang YT, Xue YR, et al. A brief review of bioactive metabolites derived from deep-sea fungi. *Marine Drugs*, 2015, 13(8): 4594–4616.
- [64] Kaleem S, Ge H, et al. Isolation, structural elucidation, and antimicrobial evaluation of the metabolites from a marine-derived fungus *Penicillium* sp. ZZ1283. *Natural Product Research*, 2019, Oct 23:1–9.
- [65] Hasan S, Ansari MI, Ahmad A, et al. Major bioactive metabolites from marine fungi. *A Review Bioinformation*. 2015 ;11(4):176-81.
- [66] Blunt JW, Copp BR, et al. Marine natural products. *Natural Product Reports* 2016, 33: 382-431.
- [67] Lucas X, Günther S. Using chiral molecules as an approach to address low-draggability recognition sites. *Computational Chemistry*, 2014, 35: 2114-2121.
- [68] Lucas X, Grüning BA, Bleher S, Günther S. The purchasable chemical space: a detailed picture. *Journal of Chemical Information and Modeling*. 2015, 55: 915-924.
- [69] Miller BW, Lim AL, et al. Shipworm symbiosis ecology-guided discovery of an antibiotic that kills colistin-resistant *Acinetobacter*. *Cell Chemical Biology*. 2021;28(11):1628–1637.
- [70] Gerwick WH, Moore BS. Lessons from the past and charting the future of marine natural products drug discovery and chemical biology. *Chemistry & Biology* 2012;19(1):85–98.

- [71] Almaliti J, Gerwick, et al. W. H. Methods in marine natural product drug discovery: what's new? *Expert Opinion on Drug Discovery*, (2023). 18(7), 687–691.
- [72] Jensen SM, Ruscetti FW, et al. Differential inhibitory effects of cyanovirin-N, griffithsin, and scytovirin on entry mediated by envelopes of gamma retroviruses and deltaretroviruses. *Virology* 2014;88(4):2327–2332
- [73] DiMasi JA, Grabowski HG, Hansen RW. Innovation in the pharmaceutical industry: new estimates of R&D costs. *Journal of Health Economics*, 2016, 47: 20–33.
- [74] Skariyachan S, Archana BA, et al. Secondary metabolites extracted from marine sponge associated *Comamonas testosteroni* and *Citrobacter freundii* as potential antimicrobials against MDR pathogens and hypothetical leads for VP40 matrix protein of Ebola virus: An in vitro and in silico investigation. *Journal of Biomolecular Structure and Dynamics*, 2016, 34(9): 1865–1883.
- [75] Nantasenamat C, Prachayasittikul V. Maximizing computational tools for successful drug discovery. *Expert Opinion on Drug Discovery*, 2015, 10(4): 321–329.
- [76] Tawfike AF, Viegelmann C, et al. Metabolomics and dereplication strategies in natural products, in metabolomics tools for natural product discovery. *Methods in Molecular Biology*, 2013, 1055: 227–244.
- [77] Sidebottom AM, Johnson AR, et al. Integrated metabolomics approach facilitates discovery of an unpredicted natural product suite from *Streptomyces coelicolor* M145. *ACS Chemical Biology*, 2013, 8(9): 2009–2016.
- [78] Roullier C, Guitton Y, et al. Automated detection of natural halogenated compounds from LC-MS profiles—application to the isolation of bioactive chlorinated compounds from marine-derived fungi. *Analytical Chemistry*, 2016, 88(18): 9143–9150.

Publisher's Note: All claims expressed in this article are solely those of the authors and do not necessarily represent those of their affiliated organizations or the publisher, the editors and the reviewers. Any product that may be evaluated in this article, or claim made by its manufacturer, is not guaranteed or endorsed by the publisher.